Pergamon

Int. J. Heat Mass Transfer. Vol. 38, No. 13, pp. 2457–2470, 1995

0017–9310/95 $9.50+0.00

0017–9310(94)00372–6

Oscillation-induced heat transport: heat transport characteristics along liquid-columns of oscillation-controlled heat transport tubes

SHIGEFUMI NISHIO, XIAO-HONG SHI and WEI-MIN ZHANG

Institute of Industrial Science, University of Tokyo, 7-22-1, Roppongi, Minato-ku, Tokyo 106, Japan

(*Received* 26 *July* 1994 *and in final form* 9 *November* 1994)

Abstract—It is known that heat transfer between two liquid-reservoirs maintained at different temperatures and connected to each other by a capillary bundle is markedly enhanced by oscillatory flow in the bundle. In this paper, first, the effects of physical properties of the working liquid on the enhanced heat flow rate are investigated. Second, the optimum operating condition maximizing the ratio of the enhanced heat flow rate to power input is examined. Finally, to increase further the ratio, a novel type with a phase shift between oscillatory flows in adjacent tubes is proposed.

1. INTRODUCTION

1.1. *Oscillation-induced heat transport*

In this paper, heat transport phenomena caused by a substance oscillating or reciprocating inside a tube or a cylinder are referred to generically as "oscillation-induced heat transport phenomena". The substance may be in solid phase, liquid phase or gas phase.

The oscillation-induced heat transport by reciprocating motion of a solid substance is observed in cryogenic refrigerators for example. Zimmerman and Longsworth [1] reported an analysis on the so-called "shuttle heat transfer" in the expander-type refrigerators which operate on the Stirling cycle, Gifford–McMahon cycle, Solvay cycle, Vuilleumier cycle, or some modification of one of these. In these refrigerators, a piston with an axial temperature gradient reciprocates inside a cylinder with a similar temperature gradient, and the reciprocating motion of the piston brings about a remarkable increase in heat flow down the temperature gradient. For example, in the expander of Gifford–McMahon refrigerators, this temperature gradient is established because one end of the displacer and cylinder is at room temperature while the other end is at a low temperature, and the enhanced heat flow from the hot to cold end due to the reciprocating motion of the displacer increases heat loss for the refrigerator. This enhanced heat transport is referred to as shuttle heat transfer. Recently, for shuttle heat transfer, Nishio and Inada [2] presented a more precise heat conduction analysis.

In the case that the oscillating substance is a liquid, the phenomena relate to the so-called "dream pipe" proposed by Kurzweg and Zhao [3]. In the dream pipe developed by them, hot and cold liquid-reservoirs are connected to each other by a capillary bundle, as shown in Fig. 1. If the liquid columns in the bundle reciprocate with an amplitude of tidal displacement smaller than the bundle length, the heat flow rate from the hot to cold reservoir is remarkably increased depending on the amplitude and frequency of the oscillatory liquid flow. Such phenomena are similar to the extraordinary mass diffusion in both steady and oscillatory viscous laminar flows within tubes which was first investigated by Taylor [4]. Since these tubes can act as heat transport tubes similar to heat pipes, the fundamental heat-transport analyses and its application have been reported recently [5–10].

In the above two cases, enhanced heat transport induced by oscillating motion of a substance inside a tube is considered to relate to temperature oscillation due to the displacement along the temperature gradient. However, if the substance is a gas, the phenomena change dramatically because temperature oscillation caused by pressure oscillation is superimposed on that due to the displacement [11]. Gifford and Longsworth [12] developed a low-temperature refrigerator without the use of low-temperature moving parts or the Joule–Thomson effect. The refrigerator consists of a cylinder, a regenerator and a mechanism causing pressure oscillation in gas inside the cylinder. Stack-type heat exchangers are located at both ends of the cylinder. In this simple refrigerator, the acoustic standing wave creates a temperature gradient along the cylinder and then an amount of heat is pumped up from the cold-end to hot-end heat exchanger. This type of refrigerator is called as the "basic pulse-tube refrigerator (PTR)", and Gifford and Longsworth [13] reported the so-called "surface pumping effect" as the fundamental mechanism of this refrigerator. Recently, modified PTRs have been developed by changing the standing wave to the traveling wave with phase shifters [14, 15].

The three examples mentioned above are generically based on heat transport induced by oscillatory

NOMENCLATURE

A area [m^2]
A_c cross-section of liquid column [m^2]
c_p specific heat of liquid [$J\ kg^{-1}K^{-1}$]
c_w specific heat of tube wall material [$J\ kg^{-1}K^{-1}$]
f frequency [s^{-1}]
$G_{os,+}$ net heat flow from hotter, stagnant boundary layer to colder core-liquid-column during half period for $X > 0$ [J]
$G_{os,-}$ net heat flow from hotter core-liquid-column to colder, stagnant boundary layer during half period for $X < 0$ [J]
H half gap of two-dimensional tube [m]
j volumetric heat generation rate [$W\ m^{-3}$]
j_0 see equation (11)
k thermal conductivity of liquid [$W\ m^{-1}K^{-1}$]
k_{ef} effective thermal conductivity [$W\ m^{-1}K^{-1}$]
$k_{ef,t}$ total, effective thermal conductivity $= k + k_{ef}$ [$W\ m^{-1}K^{-1}$]
k_w thermal conductivity of tube wall material [$W\ m^{-1}K^{-1}$]
M_u see equation (36)
$M_{\eta,op}$ see equation (32)
$M_{\kappa,op}$ see equation (31)
P amplitude of pressure gradient [$N\ m^{-3}$]
Pr Prandtl number
Q_s time-averaged, additional heat-flow-rate down unit temperature gradient $|\Omega| = 1\ K\ m^{-1}$ along tube axis [W]
Q_{os} instantaneous heat-flow-rate through slip interface [W]
$Q_{os,m}$ time-averaged heat-flow-rate through slip interface [W]
q lateral heat flux at slip interface [$W\ m^{-2}$]
q_{ax} time-averaged, axial heat flux down temperature gradient [$W\ m^{-2}$]
R tube radius [m]
S amplitude of tidal displacement of oscillatory flow [m]
t time [s]
u velocity to x direction
u_c see equation (35)
Wo Womersley number $= Wo = R\sqrt{(\omega/\nu)}$ or $H\sqrt{(\omega/\nu)}$
W_s power input to drive oscillatory flow in tube of unit length [W]
X displacement of core interface [m]
x axis along tube length [m]
y axis along gap in two-dimensional tube [m]
Z characteristic length of cross-section (R or H) [m].

Greek symbols

α $Wo\sqrt{Pr} = R\sqrt{(\omega/\kappa)}$ or $H\sqrt{(\omega/\kappa)}$
α_w $R\sqrt{(\omega/\kappa_w)}$ or $H\sqrt{(\omega/\kappa_w)}$
γ thermal diffusivity ratio $= \kappa/\kappa_w$
δ half thickness of tube wall [m]
δ_u thickness of velocity boundary layer $= \sqrt{(2\nu/\omega)}$ [m]
δ_t thermal penetration depth $= \sqrt{(2\kappa/\omega)}$ [m]
η_{sc} thermal coefficient (see equation (26))
θ temperature fluctuation in liquid [K]
θ_w temperature fluctuation in tube wall [K]
κ thermal diffusivity of liquid [$m^2\ s^{-1}$]
κ_{ef} effective thermal diffusivity [$m^2\ s^{-1}$]
$\kappa_{ef,p}$ κ_{ef} of phase shifted OCHTs [$m^2\ s^{-1}$]
κ_{ef,p^0} asymptotic value of $\kappa_{ef,p}$ for $\sigma \to 0$ [$m^2\ s^{-1}$]
$\kappa_{ef,s}$ κ_{ef} of synchronized OCHTs [$m^2\ s^{-1}$]
κ_{ef,s^0} asymptotic value of $\kappa_{ef,s}$ for $\sigma \to 0$ [$m^2\ s^{-1}$]
$\kappa_{ef,t}$ total, effective thermal diffusivity $= \kappa + \kappa_{ef}$ [$m^2\ s^{-1}$]
κ_w thermal diffusivity of tube wall material [$m^2\ s^{-1}$]
λ pressure gradient [$Pa\ m^{-1}$]
ρ density of liquid [$kg\ m^{-3}$]
ρ_w density of tube wall material [$kg\ m^{-3}$]
σ ratio of wall thickness to gap $= \delta/H$
τ time delay $= (\pi/2 - \varphi)/\omega$, see Fig. 3 [s]
χ $\sqrt{(k_w\rho_w c_w)}/\sqrt{(k\rho c_p)}$
φ phase shift between lateral heat flux and oscillatory flow, see Fig. 3
Ω axial temperature gradient [$K\ m^{-1}$]
ω angular frequency $= 2\pi f$ [s^{-1}].

Subscripts

op optimum operating condition.

Superscripts

* non-dimensional value
\# asymptotic value for $\sigma \to \infty$.

motion of a substance inside a tube. As for the latter two cases, Swift published an excellent lecture note entitled "Thermoacoustic Engines" [11]. In the present paper, however, the term "oscillation-induced heat transport" will be used to include shuttle heat transfer.

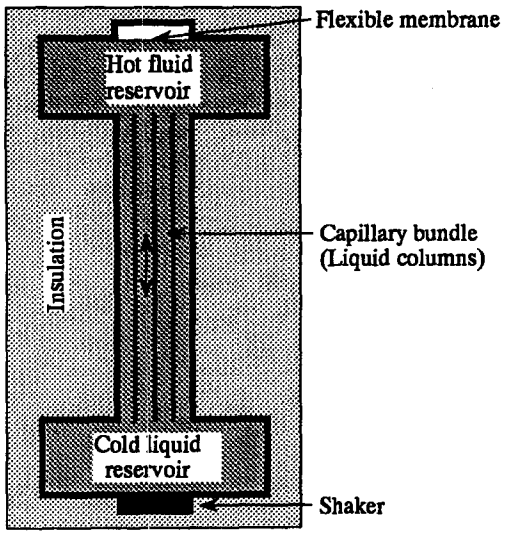

Fig. 1. Schematic diagram of dream pipe developed by Kurzweg and Zhao.

1.2. *Oscillation-controlled heat transport tube*

As stated already, the dream pipe developed by Kurzweg and Zhao [3] can act as a heat transport device similar to heat pipes. In the present paper, the heat transport devices using oscillatory liquid flows are referred to generically as "oscillation-controlled heat transport tubes (OCHTs)" to include types other than the dream pipe shown in Fig. 1. As for the OCHT shown in Fig. 1, the total, effective thermal conductivity or diffusivity in the liquid column portion is a key value to determine the thermal characteristics. Here, the total, effective thermal conductivity $k_{ef,t}$ is defined as

$$k_{ef,t} = |q_{ax}/\Omega| \tag{1}$$

where q_{ax} is the axial, time-averaged heat flux based on the cross-section of the liquid column and Ω is the temperature gradient along the liquid column. Using this definition of $k_{ef,t}$, the effective thermal conductivity k_{ef} is defined as

$$k_{ef} = k_{ef,t} - k \tag{2}$$

where k is thermal conductivity of the liquid. In the same way, the effective thermal diffusivity can be defined as

$$\kappa_{ef} = k_{ef}/\rho c_p \tag{3}$$

where ρ and c_p are density and specific heat of the liquid, respectively. In this paper, the quantities such as k_{ef} and κ_{ef} will be called as "apparent properties". As known from equations (2) and (3), the effective thermal conductivity is proportional to the effective thermal diffusivity. In the present paper, thus, thermal characteristics of OCHTs will be discussed by using k_{ef} or κ_{ef}, as the case may be.

It should be noted here that the OCHTs are based on enhanced heat transport similar to the extraordinary mass diffusion in both steady and oscillatory viscous laminar flows in which, as analyzed by Chatwin [16] and Watson [17], contaminants or gas constituents will diffuse at rates much higher than pure molecular diffusion. Thus, in the case that the effect of heat capacity of tube walls on the enhanced heat flow can be neglected, the apparent properties of OCHTs can be predicted simply by replacing mass diffusivity by thermal diffusivity in these analyses on the extraordinary mass diffusion. In the present paper, the equations obtained by such replacement in the equations derived by Watson [17] are called as the "modified Watson's equations". For such OCHTs, following Kurzweg and Zhao [3], Kurzweg [5] reported an analysis under the condition of $R^2(\omega/\kappa) < \pi$ where R is radius of the tube and ω is angular frequency of the oscillatory flow, and Ozawa and Kawamoto [6] developed a simplified numerical model to estimate the effective thermal diffusivity. Further, Katsuta *et al.* [7] reported experimental results and correlations on heat transfer between reservoirs.

On the other hand, if the effect of heat capacity of tube walls on the enhanced heat flow is not negligibly small, the apparent properties can not be predicted by the modified Watson's equations. For such cases, Tominaga [8] presented a simple formula of q_{ax} based on the thermoacoustic analysis of nonviscous fluids, and Kaviany [9] presented analyses focusing on both liquid columns and reservoirs of a bundle-type OCHT of circular tubes.

Comparing with heat pipes, OCHTs have the following features.

(1) While in heat pipes the operating temperature range is limited by the saturation temperature of the working liquid, OCHTs can enlarge the operating temperature range because they do not use phase change phenomena.

(2) While the tube material of heat pipes is limited due to material incompatibility, OCHTs are free of such limitation.

(3) While heat pipes need a special structure to produce the capillary pumping head returning the working liquid from the cold to hot end, OCHTs do not necessitate such a structure and then they are very simple.

(4) While in heat pipes a special device is needed to control the heat transport characteristics, the effective thermal conductivity or diffusivity in OCHTs can be easily controlled by changing the frequency or amplitude of the oscillatory flow.

(5) While heat pipes operate without external power supply, OCHTs need it to drive and keep the oscillatory flow.

(6) To develop compact heat transport devices, it is necessary to remove or reduce a volume to absorb the tidal displacement in OCHTs.

(7) While in heat pipes heat transfer coefficients at the hot and cold ends are very high, they should be enhanced in OCHTs.

The features (1–4) are merits of OCHTs, but (5–7) are demerits. To develop useful OCHTs, thus, such demerits should be reduced and the optimum operating condition achieving the highest performance of OCHTs should be investigated.

In the present paper, as the first paper of our study on the OCHTs, we will focus on thermal characteristics in the liquid column portion of OCHTs. First, neglecting heat capacity of tube walls, the effects of physical properties of the working liquid on the effective thermal conductivity or diffusivity along the liquid column of OCHTs will be discussed to develop the selection criteria of the working liquid. Second, introducing a concept of the thermal coefficient which is the ratio of additional heat-flow-rate to power input and also neglecting heat capacity of tube walls, the effects of geometrical and flow conditions on the thermal coefficient will be discussed to look for the optimum operating condition maximizing the coefficient. Finally, a novel phase shifted OCHT using also heat transfer through the tube walls between adjacent liquid columns will be proposed to increase further the thermal coefficient of OCHTs.

2. EFFECTS OF PHYSICAL PROPERTIES OF WORKING LIQUID

In this section, phenomenalistic key quantities controlling thermal characteristics of OCHTs will be discussed by a slip flow model to investigate the effects of physical properties of the working liquid on the effective thermal conductivity or diffusivity. In the model, to simplify the discussion, heat capacity of tube walls in OCHTs will be neglected.

2.1. *Velocity and temperature distributions in oscillatory flow*

Known as the Stokes second problem, in both steady and oscillatory viscous laminar flow in a tube of large diameter, a velocity boundary layer with a thickness roughly estimated by the following equation is formed near the tube wall [17]:

$$\delta_u = \sqrt{\left(\frac{2\nu}{\omega}\right)}. \tag{4}$$

Here, defining the Womersley number for circular tubes as

$$Wo = R\sqrt{\left(\frac{\omega}{\nu}\right)} = \frac{\sqrt{(2R)}}{\delta_u} \tag{5}$$

and for two-dimensional tubes as

$$Wo = H\sqrt{\left(\frac{\omega}{\nu}\right)} = \frac{\sqrt{(2H)}}{\delta_u} \tag{6}$$

it is known that, for $Wo \gg 1$, a 'core region' with uniform velocity appears in a central area within the cross-section of the oscillatory flow.

On the other hand, if the temperature gradient along the tube axis is kept constant, the time-averaged amount of enhanced heat flow down the axial temperature gradient due to the oscillatory flow depends on cross-sectional temperature distribution caused by the oscillatory flow [11]. In the case that heat capacity of the tube walls is negligibly small, this cross-sectional temperature distribution is generated only by the velocity profile. Here, define the non-dimensional number α for circular tubes as

$$\alpha = R\sqrt{\left(\frac{\omega}{\kappa}\right)} = \frac{\sqrt{(2R)}}{\delta_t} \tag{7}$$

and for two-dimensional tubes as

$$\alpha = H\sqrt{\left(\frac{\omega}{\kappa}\right)} = \frac{\sqrt{(2H)}}{\delta_t} \tag{8}$$

where δ_t is the thermal penetration depth defined as

$$\delta_t = \sqrt{\left(\frac{2\kappa}{\omega}\right)}. \tag{9}$$

Equations (7) and (8) indicate that, for $Wo \gg 1$ and $\alpha \gg 1$, a 'thermal-core region' with uniform temperature exists in a central area within the core region. The oscillatory flow condition corresponding to this situation is named as the 'undeveloped flow condition' in the present paper. Both the core and thermal-core regions disappear under the conditions of $Wo \ll 1$ and $\alpha \ll 1$, and then the oscillatory flow condition corresponding to this situation is named as the 'developed flow condition'.

2.2. *Slip-flow model*

Focusing on the undeveloped flow condition, we will discuss phenomenalistic key quantities governing the effective thermal conductivity or diffusivity by using a slip flow model shown in Fig. 2. In the slip flow model, for simplicity, we consider a two-dimensional tube with $2H$ gap and unit width, and we neglect heat capacity of the tube walls. The axial temperature gradient along the x axis is kept at a constant value $\Omega = \partial T/\partial x > 0$.

First, as shown in Fig. 2(a), considering a stagnant situation of the liquid column, it is divided into upper and lower liquid columns by the cross-section at $x = x_0$. Following the above definition of the axial temperature gradient, the upper liquid column is the hotter one and the lower liquid column is the colder one. For oscillatory flow situation, as shown in Fig. 2(b), it is assumed that each liquid column consists of the "stagnant boundary layer" with thickness δ_u and the "core liquid column" with uniform velocity. Therefore in the model, the hotter liquid column is subdivided into the hotter, stagnant boundary layer and the hotter core-liquid-column. In the same way, the colder liquid column is subdivided into the colder, stagnant boundary layer and the colder core-liquid-

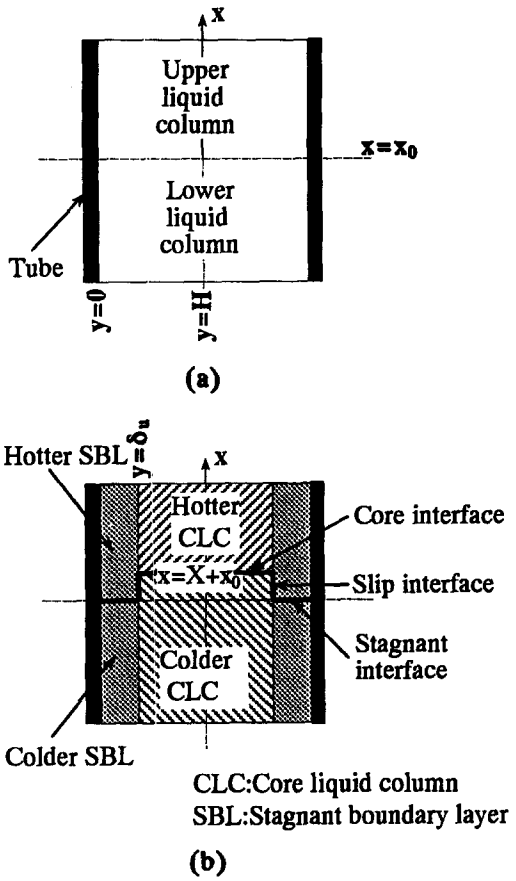

Fig. 2. Schematic diagram of slip flow model simulating thermal characteristics of OCHTs.

column. The interface between the hotter and colder stagnant boundary layers is named as the 'stagnant interface', the interface between the hotter and colder core-liquid-columns as the 'core interface', and the interface between the hotter, stagnant boundary layer and the colder core-liquid-column (or that between the colder, stagnant boundary layer and the hotter core-liquid-column) as the 'slip interface'. The location of the core interface is given by $x = X + x_0$.

The time-averaged value of total heat-flow-rate down the axial temperature gradient Ω is that from the upper to lower liquid column, and it is the sum of time-averaged heat-flow-rates through the three interfaces defined above. Since the heat flows through the stagnant and core interfaces are the axial, pure molecular-conduction heat flows down the axial temperature gradient Ω, the additional heat flow caused by the reciprocating motion of the core liquid column is only the heat flow through the slip interface normal to the reciprocating motion. The time-averaged rate of this additional, lateral heat flow, $Q_{os,m}$, relates to $G_{os,+}$ and $G_{os,-}$, where $G_{os,+}$ denotes the net heat flow from the hotter, stagnant boundary layer to the colder core-liquid-column in the half period corresponding to $X > 0$ and $G_{os,-}$ that from the hotter core-liquid-column to the colder, stagnant boundary layer in the successive half period corresponding to $X < 0$. Thus,

$$Q_{os,m} = f(G_{os,+} + G_{os,-}) \tag{10}$$

where f is frequency of the reciprocating motion of the core liquid column.

As stated above, the values of $G_{os,+}$ and $G_{os,-}$ depend on temperature distribution in the cross-section of the liquid column. Giving the reciprocating motion as $X = S \cdot \sin[\omega t]$, the temperature distribution in the cross-section at $x = x_0$ can be calculated by solving one-dimensional unsteady heat conduction along the y axis accompanied by the following volumetric heat-generation-rate in the core liquid column.

$$j_0 = -(\rho c_p)(S\Omega\omega)\cos[\omega t]. \tag{11}$$

It should be noticed here that there is a phase shift between the reciprocating motion and the heat generation rate. Denoting the temperature oscillation at $x = x_0$ by θ, the heat conduction equation in the system is given as

$$\frac{\partial\theta}{\partial t} = \kappa\frac{\partial^2\theta}{\partial y^2} + \frac{j}{\rho c_p}. \tag{12}$$

The value of j and the boundary conditions are

$$0 \leqslant y \leqslant \delta_u \quad j = 0 \tag{13}$$

$$\delta_u \leqslant y \leqslant H \quad j = j_0 \tag{14}$$

$$y = 0 \quad \text{and} \quad y = H \quad \frac{\partial\theta}{\partial y} = 0. \tag{15}$$

The time-averaged, additional heat-flow-rate from the upper to lower liquid column caused by the reciprocating motion of the core liquid column is given by

$$\begin{aligned} Q_{os,m} &= \left(\frac{\omega}{2\pi}\right)\int_0^{2\pi/\omega} Q_{os}\,dt \\ &= \left(\frac{\omega}{2\pi}\right)\int_0^{2\pi/\omega} 2qX\,dt \\ &= \left(\frac{\omega}{2\pi}\right)\int_0^{2\pi/\omega} -2k\left(\frac{\partial\theta}{\partial y}\right)_{y=\delta_u}(S\sin[\omega t])\,dt \end{aligned} \tag{16}$$

where q and Q_{os} denote the lateral heat flux and instantaneous heat-flow-rate through the slip interfaces, respectively.

One of the results for instantaneous values of X, q and Q_{os} obtained from the slip flow model is shown in Fig. 3. In Fig. 3, the working liquid is water and the oscillatory flow conditions are $S = 5$ mm and $f = 1$ Hz. The following results can be obtained from Fig. 3. First, the lateral heat flux at the slip interface, q, oscillates with the same period as the reciprocating motion, X. Second, equation (10) indicates that $Q_{os,m} = 0$ if the phase shift between the heat flux and the reciprocating motion is $\varphi = \pi/2$, but in the case of Fig. 3 this phase shift is about $\varphi = \pi/4$. In other wards,

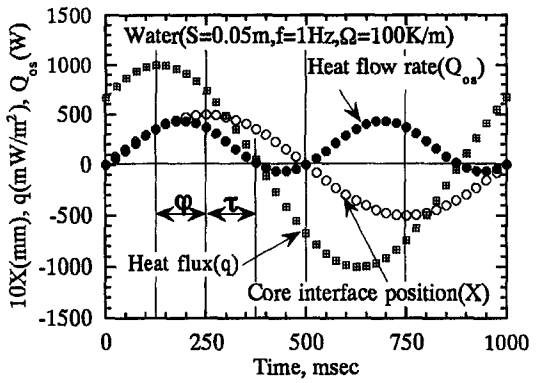

Fig. 3. Instantaneous values obtained from slip flow model.

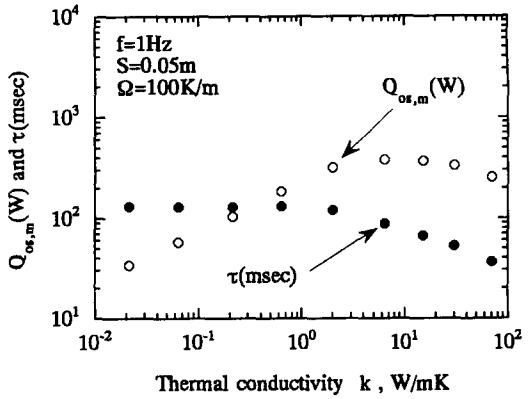

Fig. 4. Dependency of time delay and time-averaged, additional heat-flow-rate on thermal conductivity predicted from slip flow model.

focusing on the half period $0 \leqslant t \leqslant 500$ ms, the direction of the reciprocating motion changes at $t = 250$ ms, but the direction of lateral heat flow at the slip interface changes at $t = 250$ ms$+\tau$. Here, $\tau = (\pi/2-\varphi)/\omega$. This result indicates that, for the half period, the duration in which heat flows from the hotter, stagnant boundary layer to the colder core-liquid-column through the slip interface is longer by 2τ than the duration in which heat flows back from the colder core-liquid-column to the hotter, stagnant boundary layer. This phase shift φ or time delay τ results in a positive value of $G_{os,+}$. Third, the instantaneous heat-flow-rate at the slip interface, Q_{os}, oscillates with half of the reciprocating motion period and thus $G_{os,+} = G_{os,-}$. As a result, in addition to axial, pure molecular-conduction down the temperature gradient Ω, the amount of heat $2G_{os,+}$ is transported from the upper to lower liquid column during one cycle of the reciprocating motion.

The above results indicate that the phenomenalistic key quantities controlling the time-averaged, additional heat-flow-rate in both steady and oscillatory liquid flow are the phase shift between the lateral heat flux and the oscillatory flow φ and the magnitude of the lateral heat flux normal to the tube axis q. It is clear that decrease in φ and increase in q make the axial, time-averaged heat-flow-rate larger.

2.3. *Estimation of optimum working liquid*

To examine the effects of physical properties of the working liquid on the time-averaged, additional heat-flow-rate, the values of $\tau(=(\pi/2-\varphi)/\omega)$, q and $Q_{os,m}$ were calculated by changing artificially the value of thermal conductivity of the working liquid in the slip flow model. The results for τ and $Q_{os,m}$ are shown in Fig. 4. In the figure, physical properties other than thermal conductivity were taken as the respective actual values of water. As shown in the figure, the time delay τ is kept constant for smaller values of the thermal conductivity, but it starts to decrease if the thermal conductivity is increased beyond about 1 W m^{-1} K^{-1}. On the other hand, the increase in thermal conductivity makes the magnitude of the lateral heat flux at the slip interface larger (not shown in the figure). Such conflicting effects of the increase in thermal conductivity on the key quantities bring about a maximum in $Q_{os,m}$ at a value of thermal conductivity as shown in Fig. 4. Noticing that the effective thermal conductivity is given by

$$k_{ef} = \frac{Q_{os,m}}{2H\Omega} \tag{17}$$

the results shown in Fig. 4 indicate that there exists the optimum physical property of the working liquid maximizing the effective thermal conductivity or diffusivity.

Now, we will investigate quantitatively the effects of physical properties of the working liquid on the apparent quantities. Nishio *et al.* [18] reported experimental results of the effective thermal diffusivity for water in a circular tube of acryl, and they concluded that the experimental data were in good agreement with the predictions from the modified Watson's equations. For example, the modified Watson's equations for circular tubes are given as

$$\kappa_{ef} = \frac{1-\dfrac{N_1[Wo]}{N_1[\alpha]}}{2(1-Pr^{-2})N_2[Wo]}\left(\frac{S}{R}\right)^2\kappa \tag{18}$$

where

$$N[\xi] = ber^2[\xi]+bei^2[\xi] \tag{19}$$

$$N_1[\xi] = \frac{\xi N''[\xi]+N'[\xi]}{N'[\xi]} \tag{20}$$

$$N_2[\xi] = \frac{\xi^3 N[\xi]+N'[\xi]-\xi N''[\xi]-\xi^2 N'''[\xi]}{\xi^4 N'[\xi]} \tag{21}$$

and for the undeveloped flow condition

$$\kappa_{ef} = \frac{0.707}{\left(1+\dfrac{1}{Pr}\right)\left(1+\dfrac{1}{\sqrt{Pr}}\right)}\left(\frac{S^2}{R}\right)\sqrt{(\omega\kappa)} \tag{22}$$

and for the developed flow condition

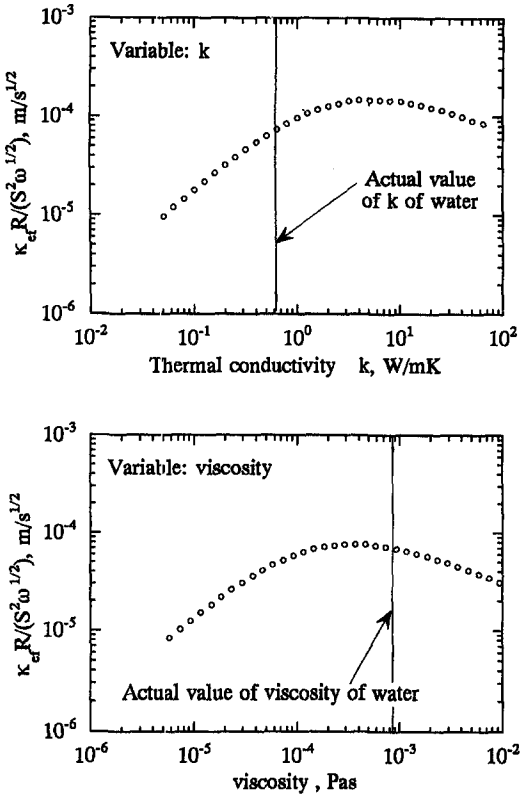

Fig. 5. Dependencies of effective thermal diffusivity on thermal conductivity and viscosity predicted from modified Watson's equations.

$$\kappa_{ef} = \frac{1}{96}\left(1 - \frac{13Pr^2+3}{2880} Wo^4\right)(RS)^2\left(\frac{\omega^2}{\kappa}\right). \quad (23)$$

Using these equations, the dependency of κ_{ef} on k (or viscosity) can be discussed by changing artificially the value of k (or viscosity) and holding other physical properties as the respective actual values of water. The results for the undeveloped flow condition are shown in Fig. 5. The vertical line is the actual value of thermal conductivity (or viscosity) of water. As well as Fig. 4, it is found that the effective thermal diffusivity reaches a maximum at a value of k (or viscosity). In addition, it is also found that the actual properties of water are near the respective optimum values.

These results can be confirmed more directly by plotting frequency characteristics of the apparent properties for a given set of S and R. In Fig. 6, the frequency characteristics predicted from equation (18) are plotted for three typical liquids. It can be found that the thermal conductivity of mercury is highest among the three liquids but the effective thermal conductivity of water is highest.

3. OPTIMUM OPERATING CONDITION

In the previous section, we discussed the effects of physical properties of the working liquid on the thermal characteristics of OCHTs and the following

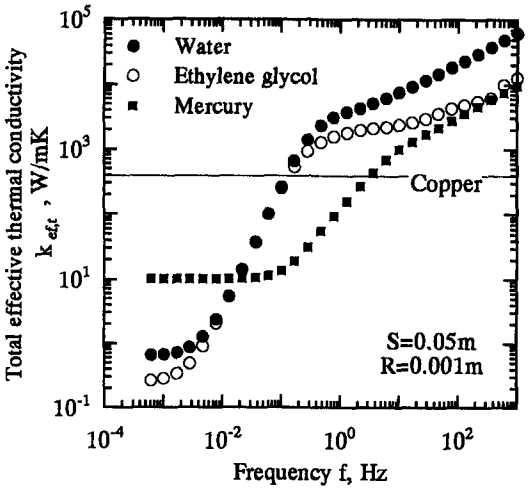

Fig. 6. Frequency characteristics of effective thermal conductivity predicted from modified Watson's equations.

results were obtained. The phenomenalistic key quantities controlling the enhanced heat-flow-rate are the phase shift between the lateral heat flux and the oscillatory flow and the magnitude of the lateral heat flux normal to the tube axis. There exists the optimum working liquid maximizing the effective thermal conductivity or diffusivity under given geometrical and oscillation conditions because of the effects of physical properties of the working liquid on the phenomenalistic key quantities. Next, in this section, introducing concepts of the 'optimum operating condition' and the 'thermal efficiency' of OCHTs, the relation between them will be discussed. Also in this section, we will neglect heat capacity of tube walls for simplicity.

3.1. *Optimum operating condition*

As known from equations (22) and (23), the increase in tube radius results in higher apparent properties under the developed flow condition, but it results in lower apparent properties under the undeveloped flow condition. This fact indicates that, if we fix the values of S and f, the apparent properties such as the effective thermal diffusivity and conductivity of a working liquid reach the respective maxima at a cross-sectional size of the tube. Since, as known from equation (18), the effective thermal diffusivity is always proportional to S^2, this cross-sectional size relates only to the frequency. In the present paper, the relation between this cross-sectional size and the frequency is named as the optimum operating condition.

Rearranging equation (18) by noticing $\alpha = \sqrt{(Pr)}Wo$, the following equation is obtained:

$$\frac{\kappa_{ef}}{\omega S^2} = \frac{1 - \dfrac{N_1[Wo]}{N_1[\alpha]}}{2(1-Pr^{-2})N_2[Wo]\alpha^2} = M_\kappa[\alpha, Pr]. \quad (24)$$

Equation (24) indicates that the optimum operating

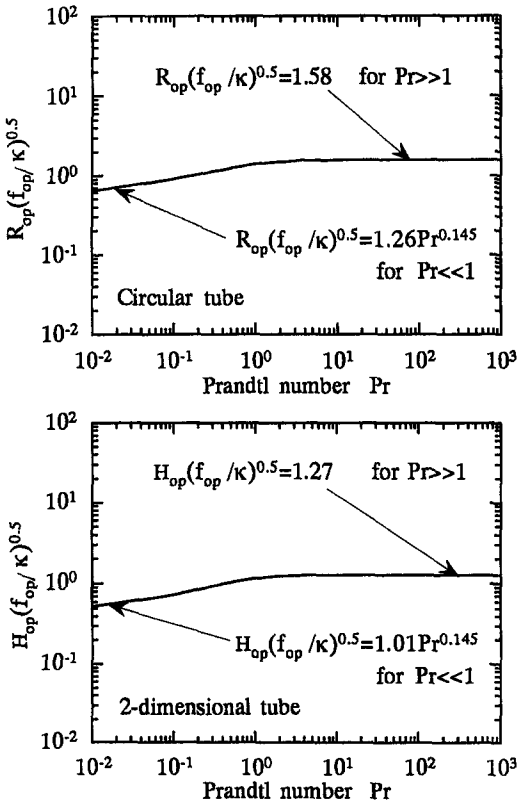

Fig. 7. Relation under optimum operating condition.

condition for a given frequency can be expressed by the following relation between α_{op} and Pr:

$$\alpha_{op} = Z_{op}\sqrt{\left(\frac{\omega_{op}}{\kappa}\right)} = \sqrt{(2\pi)}Z_{op}\sqrt{\left(\frac{f_{op}}{\kappa}\right)} = M_{op}[Pr] \tag{25}$$

where Z_{op} is the cross-sectional size ($Z_{op} = R_{op}$ for circular tubes and $Z_{op} = H_{op}$ for two-dimensional tubes) at which the effective thermal diffusivity or conductivity of a working liquid reaches a maximum for fixed values of S and ω (or f) and M_{op} is a function of Pr.

In the present paper, the values of α_{op} were numerically determined for the Prandtl number Pr by the modified Watson's equations such as equation (24), and the results are plotted in Fig. 7 together with their asymptotic expressions for $Pr \ll 1$ and $Pr \gg 1$.

3.2. *Relation of optimum operating condition to thermal coefficient of OCHTs*

Kaviany [9] proposed a concept of the efficiency of OCHTs. Following Kaviany, in the present paper, the 'thermal coefficient' of OCHTs, η_{se}, is defined by

$$\eta_{se} = \frac{Q_s}{W_s} = \frac{k_{ef}A_c}{\dfrac{\omega}{2\pi}\displaystyle\int_0^{2\pi/\omega}\int_0^{A_c}(u\cdot\lambda)\,dA\,dt} \tag{26}$$

where Q_S is the time-averaged, additional heat-flow-rate for unit temperature gradient ($|\Omega| = 1$ K m^{-1}), W_s is the power input per unit tube length driving the oscillatory flow, A_c is the cross-sectional area of the liquid column, and λ is the pressure gradient in the oscillatory flow. For example, the pressure gradient is $\lambda = P\cdot\cos[\omega t]$ for both steady and oscillatory viscous laminar flow of the tidal displacement $S\cdot\sin[\omega t]$. Referring to the modified Watson's equations, the dependencies of Q_s, W_s and η_{se} on S, Z and f are summarized as follows; for the developed flow condition in circular tubes,

$$Q_s \approx (Sf)^2R^4 \quad W_s \approx (Sf)^2 \quad \eta_{se} \approx R^4 \tag{27}$$

for the developed flow condition in two-dimensional tubes of unit width,

$$Q_s \approx (Sf)^2H^3 \quad W_s \approx (Sf)^2H^{-1} \quad \eta_{se} \approx H^4 \tag{28}$$

for the undeveloped flow condition in circular tubes,

$$Q_s \approx S^2\sqrt{(f)}R \quad W_s \approx S^2f^{2.5}R, \quad \eta_{se} \approx f^{-2} \tag{29}$$

and for the undeveloped flow condition in two-dimensional tubes of unit width,

$$Q_s \approx S^2\sqrt{f} \quad W_s \approx S^2f^{2.5} \quad \eta_{se} \approx f^{-2}. \tag{30}$$

These relations indicate that the thermal coefficient does not depend on the amplitude S and there are two typical regions for the thermal coefficient as well as k_{ef}, Q_S and W_s.

Now, let's discuss the relation between the optimum operating condition and the thermal coefficient. Figure 8 shows frequency characteristics of both the effective thermal conductivity and the thermal coefficient predicted from the modified Watson's equations for water under the condition of $S = 0.01$ m. In Fig. 8, the frequency determined by equation (25) for $R = R_{op} = 0.4$ mm, f_{op}, is also shown. In the figure, the effective thermal conductivity obtained at $R = R_{op}$ and $f = f_{op}$ is denoted by k_0. If the working liquid and the amplitude of tidal displacement of the oscillatory flow are fixed, this value k_0 is also obtained, for example, at $f = f_{lf}$ for $R = 0.1$ mm ($< R_{op}$) and at f_{hf} for $R = 1$ mm ($> R_{op}$) as shown in Fig. 8. Here, comparing $\eta_{se}[R_{op}, f_{op}]$ with $\eta_{se}[R = 0.1\text{ mm}, f_{lf}]$ and $\eta_{se}[R = 1\text{ mm}, f_{hf}]$ in Fig. 8, it is found that $\eta_{se}[R = R_0, f_{op}]$ is higher than both $\eta_{se}[R = 0.1\text{ mm}, f_{lf}]$ and $\eta_{se}[R = 1\text{ mm}, f_{hf}]$. It can be, thus, concluded that, to obtain a certain value of the effective thermal conductivity or diffusivity for a given amplitude of tidal displacement of oscillatory flow, the highest thermal coefficient is achieved under the optimum operating condition.

In the above discussion, we fixed the amplitude S to obtain the value of k_0. As shown in Figs. 9 and 10, however, we can discuss the relation between the effective thermal conductivity and the thermal

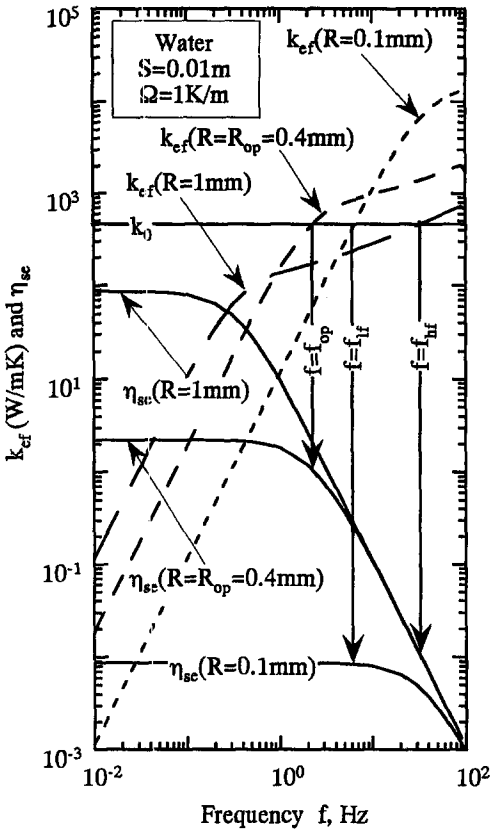

Fig. 8. Relation between optimum operating condition and thermal efficiency at fixed amplitude.

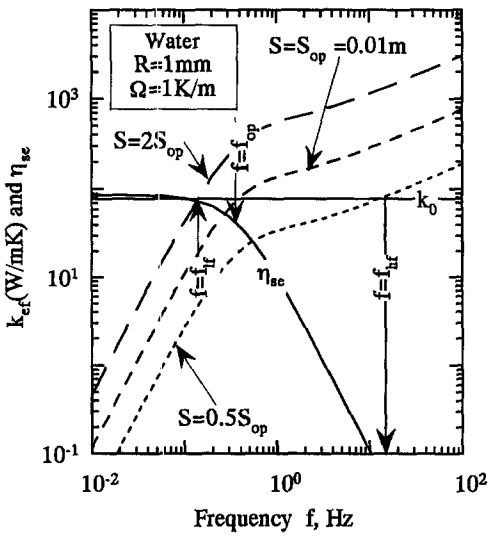

Fig. 9. Relation between optimum operating condition and thermal efficiency at fixed tube radius.

coefficient also by fixing the cross-sectional size or the frequency. Here, it should be noted that only one curve is plotted for the thermal coefficient in Figs. 9 and 10 because the thermal coefficient does not depend on S as known from equations (27)–(30). In Fig. 9, the tube radius is fixed at $R = 1$ mm and the frequency

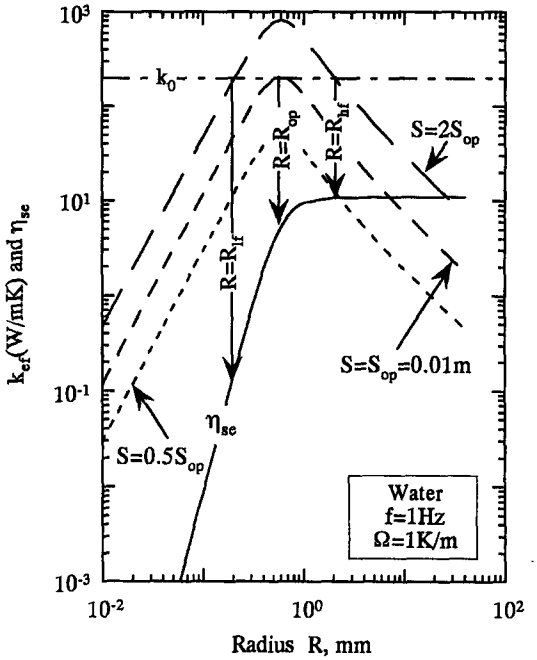

Fig. 10. Relation between optimum operating condition and thermal efficiency at fixed frequency.

under the optimum operating condition for $R = 1$ mm is denoted by f_{op}. The value of k_0 is achieved by the amplitude S_{op} under the optimum operating condition. In this case, the value of k_0 is also obtained at f_{lf} for $S = 2S_{op}$ and f_{hf} for $0.5S_{op}$ for example. As can be seen from Fig. 9, in this case, a high thermal coefficient is achieved if we choose a frequency smaller than the frequency determined by the optimum operating condition (that is, $f < f_{op}$). In the same way, it is found from Fig. 10 that, in the case that the frequency is given, a high thermal coefficient is obtained if we choose a radius larger than the radius determined by the optimum operating condition (that is, $R > R_{op}$). So far, we have examined the relation between the optimum operating condition and the thermal coefficient for circular tubes, but the same results are obtained for two-dimensional tubes.

3.3. *Key values obtained at optimum operating condition*

As shown in Sections 3.1 and 3.2, the optimum operating condition is very important to achieve high thermal coefficients in OCHTs. Next, the values of κ_{ef} and η_{se} obtained under the optimum operating condition, $\kappa_{ef,op}$ and $\eta_{se,op}$, will be examined by using the modified Watson's equations.

Using equations (24) and (25), the effective thermal diffusivity obtained at the optimum operating condition, $\kappa_{ef,op}$, can be expressed as

$$\kappa_{ef,op} = M_{\kappa,op}[Pr](\omega_{op}S^2). \tag{31}$$

In the same way, the thermal coefficient obtained at the optimum operating condition can be expressed as

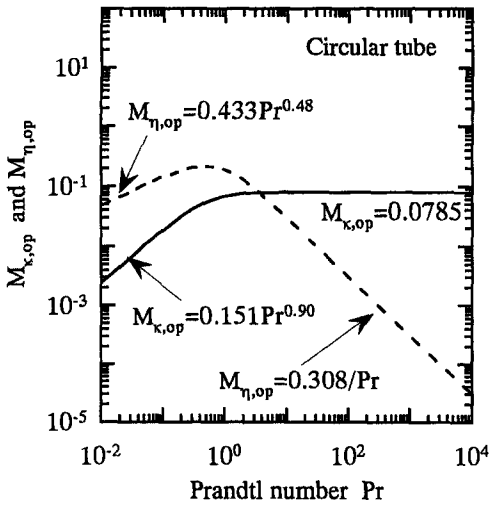

Fig. 11. Coefficients for effective thermal diffusivity and thermal coefficient obtained under optimum operating condition.

$$\eta_{se,op} = M_{\eta,op}[Pr]\left(\frac{c_p\Omega}{\omega_{op}^2 L}\right) \tag{32}$$

where $\Omega = 1\ \mathrm{K\ m^{-1}}$ and the tube length $L = 1$ m from the definition of η_{se}. Using the results on the optimum operating condition shown in Fig. 7 and also the modified Watson's equations such as equations (18)–(21), the values of $M_{\kappa,op}$ and $M_{\kappa,op}$ were numerically calculated and the results are plotted in Fig. 11 for circular tubes as an example. As shown in the figure, the maximum value of $M_{\kappa,op}$ is 0.0782 and it is achieved for about $Pr > 1$. On the other hand, the value of $M_{\eta,op}$ reaches the maximum at about $Pr = 1$. These results indicate that liquids of $Pr \cong 1$ are near the optimum working liquid for OCHTs.

4. EFFECTS OF HEAT TRANSFER AT/THROUGH TUBE WALL

In the previous sections, we discussed thermal characteristics of OCHTs by neglecting heat capacity of the tube walls and it was found that the optimum operating condition gives a measure to achieve high thermal coefficients. However, as shown by Kaviany [9] for circular tubes, heat capacity of the tube walls can increase the apparent properties of OCHTs. On the other hand, the increase in wall thickness brings about increase in total cross-section of OCHTs and then it reduces the nominal, apparent properties defined by the total cross-section including the tube walls. In this section, we propose a novel OCHT which can increase the effective thermal conductivity or diffusivity by using heat transfer through the tube wall without adding thick tube walls to OCHTs.

4.1. *Phase shifted OCHTs*

Since the amount of axial heat flow in a single OCHT is not so large, the OCHT must be used as a bundle, as shown in Fig. 1. In this section, thus, thermal characteristics of bundle type OCHTs will be discussed. For simplicity, we selected a two-dimensional bundle shown in Fig. 12. The gap filled with liquid is $2H$ and the wall thickness is 2δ. The tidal displacement of oscillatory flow in liquid column A in Fig. 12 is given as $S\cdot\sin[\omega t]$. As for the oscillatory flows in liquid columns B and C, it is possible to consider the following typical situations. In the first case, these liquid columns oscillate in phase with liquid column A. In the second case, both liquid columns B and C oscillate as $-S\cdot\sin[\omega t]$. The former is the conventional type and it is named the 'synchronized OCHTs' in the present paper. The latter is the novel type proposed in the present paper and it is named the 'phase shifted OCHTs'. An example of the phase shifted OCHTs is shown in Fig. 13. It should be noted here that the structure shown in Fig. 13 can also reduce or remove the volume to absorb the tidal displacement of oscillatory flow.

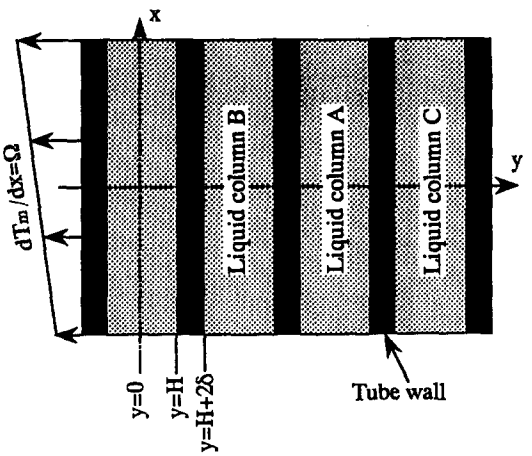

Fig. 12. Schematic diagram of phase shifted OCHT in two-dimensional tubes.

Since, focusing on the central portion of the tube length of these OCHTs, power input driving oscillatory flow in the phase-shifted OCHTs is the same with that in the synchronized OCHTs, in this section only the thermal characteristics in the synchronized and phase shifted OCHTs will be discussed.

4.2. *Analysis of effective thermal diffusivity or conductivity in phase shifted OCHTs*

Supposing both steady and oscillatory viscous laminar flow in a two-dimensional tube and also giving its

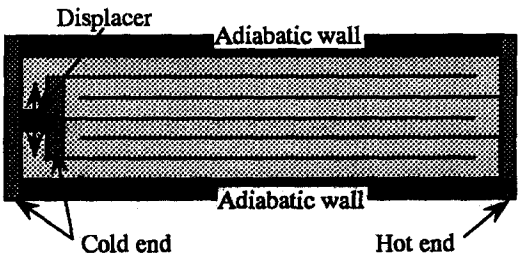

Fig. 13. Example of phase shifted OCHTs.

pressure gradient along the tube axis by $P\cdot\cos[\omega t]$, the instantaneous velocity distribution $u[t;y]$ is given by the following equations [18]:

$$u[y^*;t] = \mathrm{Re}\{u_c F[y^*]\exp[i\omega t]\} \tag{33}$$

$$F[y^*] = i\left(\frac{\cosh[\sqrt{(i)}Woy^*]}{\cos[\sqrt{(i)}Wo]} - 1\right) \tag{34}$$

where

$$u_c = \frac{P}{\rho\omega} = \frac{\omega S}{\sqrt{(1-M_u)}} \tag{35}$$

$$M_u = \frac{2(\beta\sinh[\beta]+\beta\sin[\beta]-\cosh[\beta]+\cos[\beta])}{\beta^2(\cosh[\beta]+\cos[\beta])} \tag{36}$$

$$y^* = \frac{y}{H}, \quad \beta = \sqrt{(2)}Wo \tag{37}$$

In equations (33) and (34) 'i' denotes the imaginary unit and $\mathrm{Re}\{X\}$ the real part of the complex X.

Next, to determine the instantaneous temperature distribution, the following assumptions were employed; all physical properties of the liquid and tube material are constant and viscous heating in the liquid is negligible. Denoting the temperature fluctuation in liquid by θ and the time-averaged temperature at $x = x_0$ by T_m, the instantaneous temperature at $x = x_0$ is given by $T = T_m + \theta$. Noticing $\partial\theta/\partial x = 0$ for both steady and oscillatory flow condition, the energy equation for the liquid becomes

$$\frac{\partial\theta}{\partial t} + u\Omega = \kappa\frac{\partial^2\theta}{\partial y^2}. \tag{38}$$

In the same way, denoting the temperature fluctuation in the walls by θ_w, the energy equation for the tube walls becomes

$$\frac{\partial\theta_w}{\partial t} = \kappa_w\frac{\partial^2\theta_w}{\partial y^2}. \tag{39}$$

For the phase shifted OCHTs, the boundary conditions are

$$y = 0 \quad \frac{\partial\theta}{\partial y} = 0 \tag{40}$$

$$y = H \quad \theta[y;t] = \theta_w[y;t] \quad k\frac{\partial\theta}{\partial y} = k_w\frac{\partial\theta_w}{\partial y} \tag{41}$$

$$y = H+\delta \quad \theta_w[y;t] = 0. \tag{42}$$

The boundary condition (42) is derived from the fact $\theta_w[H+\varepsilon;t] = -\theta_w[H+2\delta-\varepsilon;t]$ for the phase shifted OCHTs where $1 < \varepsilon < \delta$.

Both θ and θ_w fluctuate with the angular frequency ω and their amplitudes are proportional to Ω and S. Using equation (35), thus, the solutions can be assumed as

$$\theta = \frac{\Omega u_c}{\omega}G[y]\exp[i\omega t] \tag{43}$$

$$\theta_w = \frac{\Omega u_c}{\omega}G_w[y]\exp[i\omega t]. \tag{44}$$

Substituting equations (43) and (44) for (38) and (39), and using equations (40)–(42), the solutions are

$$G[y^*;t] = 1 + A\cdot\cosh[\sqrt{(i)}Woy^*] + B\cdot\cosh[\sqrt{(i)}\alpha y^*] \tag{45}$$

$$G_w[y^*;t] = C(\cosh[\sqrt{(i)}\alpha_w y^*] - D\cdot\sinh[\sqrt{(i)}\alpha_w y^*]) \tag{46}$$

where

$$A = \frac{Pr}{(1-Pr)\cosh[\sqrt{(i)}Wo]} \tag{47}$$

$$B = \left(\frac{B_{11}}{B_{12}}\right)(1 - D\cdot\tanh[\sqrt{(i)}\alpha_w]) - B_2 \tag{48}$$

$$B_{11} = \mu(\sqrt{(Pr)}\tanh[\sqrt{(i)}Wo] - \tanh[\sqrt{(i)}\alpha]) \tag{49}$$

$$B_{12} = (1-Pr)\{\mu\sinh[\sqrt{(i)}\alpha](D\cdot\tanh[\sqrt{(i)}\alpha_w] - 1) + \sqrt{(\gamma)}\cosh[\sqrt{(i)}\alpha](\tanh[\sqrt{(i)}\alpha_w] - D)\} \tag{50}$$

$$B_2 = \frac{1}{(1-Pr)\cosh[\sqrt{(i)}\alpha]} \tag{51}$$

$$C = \left(\frac{B_{11}}{B_{12}}\right)\frac{\cosh[\sqrt{(i)}\alpha]}{\cosh[\sqrt{(i)}\alpha_w]} \tag{52}$$

$$D = \coth[\sqrt{(i)(1+\sigma)}\alpha_w] \tag{53}$$

and

$$\alpha_w = \sqrt{(\gamma)}\alpha, \quad \sigma = \frac{\delta}{H} \quad \mu = \frac{k}{k_w} \quad \gamma = \frac{\kappa}{\kappa_w}.$$

When $\sigma \to \infty$ we find from equations (48)–(53) that B approaches

$$B^* = -\left(\frac{Pr}{(1-Pr)\cosh[\sqrt{(i)}\alpha]}\right) \times \left(\frac{\sqrt{(Pr)}\tanh[\sqrt{(i)}Wo]+\chi}{\tanh[\sqrt{(i)}\alpha]+\chi}\right) \tag{54}$$

and when $\sigma \to 0$

$$B_{0,p} = -\frac{1}{(1-Pr)\cosh[\sqrt{(i)}\alpha]}. \tag{55}$$

Using equations (33), (35) and (43), the time-averaged, total heat flux down the axial temperature gradient at y in the cross-section of the liquid column, q_{ax}, can be given by

$$q_{ax} = k|\Omega| + \left(\frac{\omega}{2\pi}\right)\int_0^{2\pi/\omega}\rho c_p\,\mathrm{Re}\{u\}\,\mathrm{Re}\{\theta\}\,dt$$

$$= |\Omega|\left\{k + \left(\frac{\rho c_p}{2}\right)\left(\frac{u_c^2}{\omega}\right)\mathrm{Re}\{F\cdot G^+\}\right\}$$

$$= |\Omega|\left\{k+\left(\frac{\rho c_p}{2}\right)\left(\frac{\omega S^2}{1-M_u}\right)\mathrm{Re}\{F\cdot G^+\}\right\} \quad (56)$$

where G^+ denotes the complex conjugation of G. Finally, using equations (33)–(37), (45)–(53) and (56), the effective thermal diffusivity averaged over the cross-section of the liquid column is given by

$$\kappa_{ef} = \left(\frac{1}{\rho c_p |\Omega|}\right)\int_0^1 \frac{\rho c_p |\Omega|}{2}\left(\frac{\omega S^2}{1-M_u}\right)\mathrm{Re}\{F\cdot G^+\}\,dy^*$$

$$= \left\{\frac{\omega S^2}{2(1-M_u)}\right\}\int_0^1 \mathrm{Re}\{F\cdot G^+\}\,dy^*$$

$$= \omega S^2 \kappa_{ef}^* \quad (57)$$

where κ_{ef}^* is non-dimensional thermal diffusivity. The total, effective thermal diffusivity is given by

$$\kappa_{ef,t} = \kappa + \kappa_{ef}. \quad (58)$$

4.3. *Analysis of effective thermal conductivity in synchronized OCHTs*

As for the synchronized OCHTs, since temperature distribution is symmetric for the mid plane of the tube wall, the boundary condition (42) becomes

$$y = H+\delta;\frac{\partial\theta}{\partial t} = 0. \quad (59)$$

Since other equations and conditions are the same as those for the phase shifted OCHTs, it is found that the solutions for the phase shifted OCHTs can be used if equation (53) is replaced by

$$D = \tanh[\sqrt{(i)}(1+\sigma)\alpha_w]. \quad (60)$$

In this case, when $\sigma \to 0$, B approaches

$$B_{0,s} = -\frac{\sqrt{(Pr)}\tanh[\sqrt{(i)Wo}]}{(1-Pr)\sinh[\sqrt{(i)}\alpha]}. \quad (61)$$

4.4. *Thermal characteristics of phase shifted OCHTs*

From equations (33)–(37), (45)–(53) and (57), it is found that the non-dimensional, effective thermal diffusivity, κ_{ef}^*, is a function of Pr, Wo, $\mu(=k/k_w)$, $\gamma(=\kappa/\kappa_w)$ and $\sigma(=\delta/H)$ and the effects of these parameters on κ_{ef}^* are complicated. In this paper, thus, the effects of these parameters on κ_{ef}^* are examined for water.

The non-dimensional, effective thermal diffusivities of water for $\gamma = 0.01$ and $\gamma = 1$ are plotted to the non-dimensional wall thickness σ in Figs. 14 and 15, respectively. The parameters in each figure are the Womersley number Wo and the thermal conductivity ratio μ. In each figure, the non-dimensional, effective thermal diffusivity of the synchronized OCHTs is denoted by $\kappa_{ef,s}^*$ and that of the phase shifted OCHTs by $\kappa_{ef,p}^*$.

From the figures, it is found that the asymptotic values in the two types for $\sigma \to 0$, $\kappa_{ef,s}^* = \kappa_{ef,s0}^*$ and $\kappa_{ef,p}^* = \kappa_{ef,p0}^*$, depend on Wo but not on μ. These

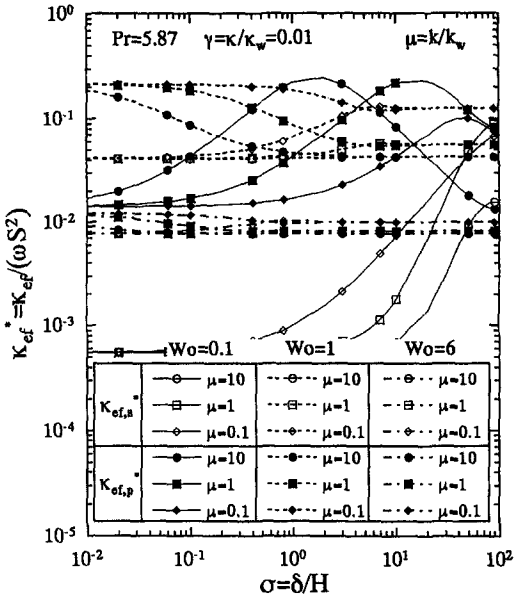

Fig. 14. Comparison between thermal characteristics of synchronized and phase shifted OCHTs ($\gamma = 0.01$).

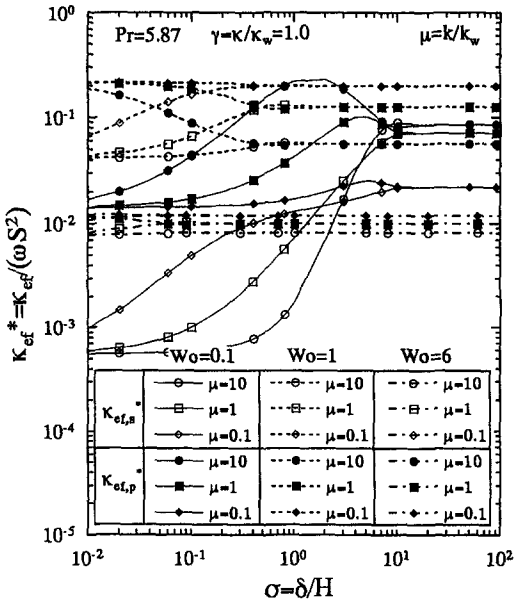

Fig. 15. Comparison between thermal characteristics of synchronized and phase shifted OCHTs ($\gamma = 1.0$).

asymptotic values correspond to the non-dimensional, effective thermal diffusivity for tube walls of negligibly small heat capacity, and the asymptotic value $\kappa_{ef,s0}^*$ corresponds to the effective thermal diffusivity predicted from the modified Watson's equations. On the other hand, for $\sigma \to \infty$, the non-dimensional, effective thermal diffusivities in both types reach another asymptotic value at $\sigma = \sigma^*$. From comparison between Figs. 14 and 15, it is found that the value of σ^* depends on Pr, Wo and γ but not on μ. As is

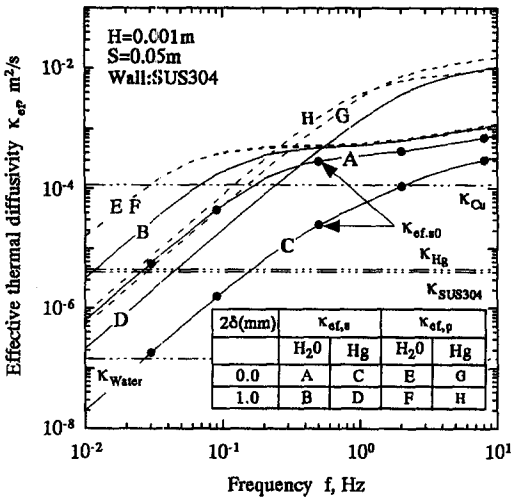

Fig. 16. Comparison between frequency characteristics of effective thermal diffusivity of synchronized and phase shifted OCHTs.

known, the asymptotic values of the two types for $\sigma \to \infty$ are independent of the type of OCHTs and then a unique value $\kappa_{ef}^{*\#}$.

As σ increases with keeping other parameters constants, the value of $\kappa_{ef,s}^{*}$ increases almost monotonously from $\kappa_{ef,s0}^{*}$ to $\kappa_{ef}^{*\#}$, while a small maximum is observed near $\sigma = \sigma\#$. As for the phase shifted OCHTs, with increase of σ, the value of $\kappa_{ef,p}^{*}$ decreases monotonously from $\kappa_{ef,p0}^{*}$ to $\kappa_{ef}^{*\#}$ for larger values of Wo. For smaller values of Wo, with increase of σ, it increases from $\kappa_{ef,p0}^{*}$ and reaches the asymptotic value $\kappa_{ef}^{*\#}$ through a maximum. In addition, as known from Figs. 14 and 15, the values of $\kappa_{ef,p}^{*}$ for smaller values of σ are independent of γ.

For smaller values of Wo (for example, $Wo = 0.1$ in the figures), $\kappa_{ef,p0}^{*}$ is much higher than $\kappa_{ef,s0}^{*}$. In the synchronized OCHTs, while $\kappa_{ef,s}^{*}$ can be higher than $\kappa_{ef,s0}^{*}$ if a thick wall is added to the system, the nominal values of $\kappa_{ef,s}^{*}$ based on the total cross-section cannot be so high because $\sigma^{*} \cong 10$. On the other hand, in the phase shifted OCHTs, $\kappa_{ef,p}^{*}$ reach a maximum at $\sigma \cong 1$. Summarizing these results, it can be concluded that, for smaller values of Wo, the phase shifted OCHTs can achieve effective thermal diffusivities or conductivities much higher than those of the synchronized OCHTs without adding thick walls.

The ratio of $\kappa_{ef,p0}^{*}$ to $\kappa_{ef,s0}^{*}$ for a given Wo decreases with increase of Wo. For medium values of Wo (for example, $Wo = 1$ in the figures), however, $\kappa_{ef,p0}^{*}$ is still much higher than $\kappa_{ef,s0}^{*}$. This results also confirm the superiority of the phase shifted OCHTs to the conventional synchronized OCHTs.

To illustrate the superiority of the phase shifted OCHTs more directly, the frequency characteristics of the effective thermal diffusivity are plotted for the two types of OCHTs of $2H = 2$ mm and $S = 5$ cm in Fig. 16. In the figure, solid line A represents the synchronized OCHT with very thin walls for water, and solid line C for mercury. Solid lines B and D represent the synchronized OCHTs with $\delta = 1$ mm for water and mercury, respectively. Comparison among these lines indicates that, as Kaviany [9] reported for circular tubes, the effective thermal conductivity of the synchronized OCHTs cannot be increased without adding thick walls. The effect of wall thickness is strong, especially in the case of mercury whose Prandtl number is small. Dotted line E represents the phase shifted OCHT with very thin walls for water, and dotted line G for mercury. Dotted lines F and H represent the phase shifted OCHTs with $\delta = 1$ mm for water and mercury, respectively. From comparison among these lines, it is found that, in the phase shifted OCHTs, the effect of wall thickness on $k_{ef,p}$ is very weak and the phase shifted OCHTs can achieve effective thermal conductivities and thermal coefficients much higher than those of the synchronized OCHTs.

5. CONCLUSIONS

In the present paper, we discussed how to increase the thermal coefficient in oscillation-controlled heat transport tubes (OCHTs) and we obtained the following conclusions.

(1) In the undeveloped flow condition within tubes of negligibly small heat capacity, the phenomenalistic key values controlling the thermal characteristics of OCHTs are the phase shift between the lateral heat flux and the oscillatory flow and the magnitude of the lateral heat flux. Decrease in the phase shift and increase in the magnitude of lateral heat flux result in higher effective thermal conductivities or diffusivities. Increase in thermal conductivity of the working liquid brings about higher lateral heat fluxes but it results in larger phase shifts. Because of such conflicting effects, there exists the optimum working liquid maximizing the effective thermal conductivity or diffusivity under fixed geometrical and oscillation conditions. Water is a candidate for the optimum working liquid.

(2) If the amplitude and frequency of oscillatory flow are fixed, there is a relation between the frequency and the cross-sectional size (for example, radius for circular tubes) under which the effective thermal conductivity or diffusivity of OCHTs with tubes of negligibly small heat capacity reaches a maximum. This relation, that is the optimum operating condition, can be expressed as a relation between α and Pr. The optimum operating condition relates also to the measure to achieve higher thermal coefficients of OCHTs. Here, the thermal coefficient is the ratio of the time-averaged, additional heat-flow-rate resulting from oscillatory flow to the input power driving the oscillatory flow. Liquids of $Pr \cong 1$ are the optimum operating liquid which maximizes the effective thermal diffusivity (or conductivity) and can achieve higher thermal coefficients for OCHTs under the optimum operating condition.

(3) While in the conventional synchronized

OCHTs the thermal coefficient can be increased by adding thick tube walls, the phase shifted OCHTs proposed in the present paper can achieve much higher thermal coefficients without adding thick walls and also can remove or reduce a volume to absorb the tidal displacement of oscillatory flow.

REFERENCES

1. F. J. Zimmerman and R. C. Longsworth, Shuttle heat transfer, *Adv. Cryognic Engng* **16,** 342–351 (1970).
2. S. Nishio and T. Inada, Shuttle heat transfer in refrigerators. In *Transport Phenomena in Thermal Engineering* (ISTP-6), Vol. 1, pp. 484–489. Begell House, New York (1993).
3. U. H. Kurzweg and L. Zhao, Heat transfer by high-frequency oscillations: a new hydrodynamic technique for achieving large effective thermal conductivities, *Phys. Fluids* **27,** 2624–2627 (1984).
4. G. I. Taylor, Dispersion of soluble matter in solvent flowing slowly through a pipe, *Proc. R. Soc. Lond.* **A219,** 186–203 (1953).
5. U. H. Kurzweg, Enhanced heat conduction in fluids subjected to sinusoidal oscillations, *ASME J. Heat Transfer* **107,** 459–462 (1985).
6. M. Ozawa and A. Kawamoto, Lumped-parameter modeling of heat transfer enhanced by sinusoidal motion of fluid, *Int. J. Heat Mass Transfer* **34,** 3083–3095 (1991).
7. M. Katsuta, K. Nagata, Y. Maruyama and A. Tsujimori, Fundamental characteristics of heat conduction enhancement in oscillating viscous flow-Dream pipe, *Proceedings of ASME–JSME Thermal Engineering Joint Conference*, Vol. 3, pp. 69–74 (1991).
8. A. Tominaga, Heat transport mechanism of dream pipe, *Cryogenic Engng.* **25,** 300–303 (1990) (in Japanese).
9. M. Kaviany, Performance of a heat exchanger based on enhanced heat diffusion in fluids by oscillation: analysis, *ASME J. Heat Transfer* **112,** 49–55 (1990).
10. M. Kaviany and M. Reckker, Performance of a heat exchanger based on enhanced heat diffusion in fluids by oscillation: experiment, *ASME J. Heat Transfer* **112,** 56–63 (1990).
11. G. W. Swift, Thermoacoustic engines, *J. Acoust. Soc. Am.* **84,** 1145–1180 (1988).
12. W. E. Gifford and R. C. Longsworth, Pulse tube refrigeration, ASME Paper No. 63-WA-290, presented at Winter Annual Meeting of ASME, Philadelphia (1963).
13. W. E. Gifford and R. C. Longsworth, Surface heat pumping, *Adv. Cryogenic Engng* **11,** 171–179 (1966).
14. E. I. Mikulin, A. A. Tarasov and M. P. Shkrebyonock, Low temperature expansion pulse tubes, *Adv. Cryogenic Engng* **29,** 629–637 (1984).
15. S. Zhu, P. Wu, Z. Chen and Y. Zhou, A single stage double inlet pulse tube refrigerator capable of reaching 42K, *Cryogenics* **30** (September suppl.), 257–261 (1990).
16. P. C. Chatwin, On the longitudinal dispersion of passive contaminant in oscillatory flows in tubes, *J. Fluid Mech.* **71,** 513–527 (1975).
17. E. J. Watson, Diffusion in oscillatory pipe flow, *J. Fluid Mech.* **133,** 233–244 (1983).
18. S. Nishio, M. Honma and W. M. Zhang, Oscillation-controlled heat transport tube (1st report, effect of liquid properties), *Trans. JSME Ser. B* **60,** 233–239 (1994) (in Japanese).